Supporting Information

Hyperfine Coupling to the Bridging ^{17}O in the di-μ-oxo Core of a Mn^{III}-Mn^{IV} Model Significant to the Core Electronic Structure of the O$_2$-evolving Complex in Photosystem II

Oleg M. Usov, Vladimir M. Grigoryants, Ranitendranath Tagore, Gary W. Brudvig,

and Charles P. Scholes

Overview

Part 1, pages S2–S5, provides information on the preparation of di-μ-oxo Mn^{III}-Mn^{IV} bipyridyl dimers in a 1:1 CH$_3$CN-DMF glass and on the EPR spectra obtained from that glass. The EPR features of the di-μ-oxo Mn^{III}-Mn^{IV} bipyridyl dimers in CH$_3$CN-DMF glass were sharper than those in the CH$_3$CN-CH$_2$Cl$_2$ glass, the ENDOR features in both glasses were comparable, but the DMF did give rise to a Mn^{II} impurity.

Part 2, pages S6–S11, provides a comparison of line broadening simulations due to a Gaussian packet, a di-^{17}O 1:2:3:4:5:6:5:4:3:2:1 packet, and to a mono-^{17}O 1:1:1:1:1:1 packet. These simulations are applied to the second derivative X-band EPR data 300-600 Gauss above the EPR line center for the di-μ-oxo-Mn^{III}-Mn^{IV} bipyridyl dimer in both the CH$_3$CN-CH$_2$Cl$_2$ and CH$_3$CN-DMF glasses. These line broadening simulations showed that the hyperfine coupling which accounts for the ENDOR ^{17}O results best accounts for the EPR broadening if there are two, rather than one, equivalent di-μ-oxo ^{17}O atoms.

Part 1

As previously indicated, a CH_3CN (HPLC grade, Fisher) solution 2.5 mM in Mn^{III}-Mn^{IV} bipyridyl dimer was initially prepared, and trace H_2O, either as $H_2{}^{16}O$ or as isotopically enriched $H_2{}^{17}O$ (84 % atomic enrichment in ^{17}O, Isotec.), was added at 1 μL water to 200 μL CH_3CN. At this point DMF (dimethylformamide (Fisher HPLC grade, freshly opened) was added and the sample immediately frozen. A transparent glass, superior to the CH_3CN-CH_2Cl_2 glass in optical clarity and sharpness of many EPR features, was formed. However, as shown in Figure 1S, there was evidence near g = 2.00 (3400 Gauss at X-band) for additional EPR features indicating Mn^{II} contamination. The Mn^{III}-Mn^{IV} bipyridyl dimer is an oxidizing species and even fresh HPLC grade DMF may contain reducing impurities; the end result is that one must exercise care that the solvent does not reduce di-μ-oxo Mn^{III}-Mn^{IV} to Mn^{II}. Such Mn^{II} was not observed with the CH_3CN-CH_2Cl_2 glass and was not reported in previous studies of Mn^{III}-Mn^{IV} bipyridyl dimers.[1,2]

The outlying features, particularly those 300-600 Gauss above the line center, were unperturbed by the Mn^{II}, and these features provided through EPR, as shown in Figures 2S and 3S, excellent evidence for the ^{17}O line broadening brought on by exchange of ^{17}O from isotopically enriched $H_2{}^{17}O$. Figure 3S shows the efficacy of convoluting the narrow line spectrum from the ^{16}O dimer with a Gaussian broadening function to simulate the experimental ^{17}O dimer spectrum and, through the relation of the Gaussian packet width to the ^{17}O hyperfine coupling, to estimate the di-μ-oxo ^{17}O hyperfine coupling. (That relation is given in Footnote 16 in the body of this Communication, where the root mean square width between derivative extrema in the Gaussian line shape would be $2A[\mathbf{n}I(I+1)/3]^{1/2} = 4.84 \cdot |^{17}\mathbf{A}|$, when $\mathbf{n}$ = 2 and I = 5/2.)

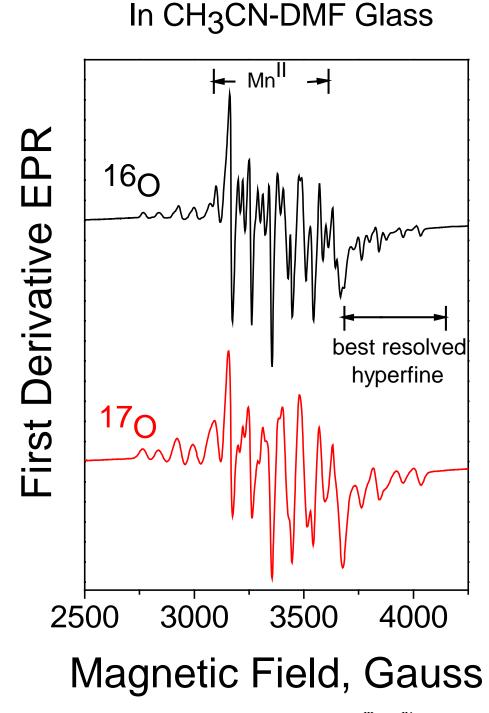**Figure 1S.** First-derivative X-band EPR spectra of di-μ-oxo Mn^{III}-Mn^{IV} bipyridyl dimers exchanged with $H_2{}^{16}O$ (black) and $H_2{}^{17}O$ (red) in CH_3CN-DMF, recorded at T = 15 K, 6 Gauss field modulation, 100 s signal averaging with a 2000 Gauss field sweep, 2 mW microwave power, EPR frequency= 9.525 GHz.. The noted central region shows evidence of Mn^{II} contamination. The high field region provides the best hyperfine detail and is most sensitive to ^{17}O broadening – see Figures 2S and 3S.
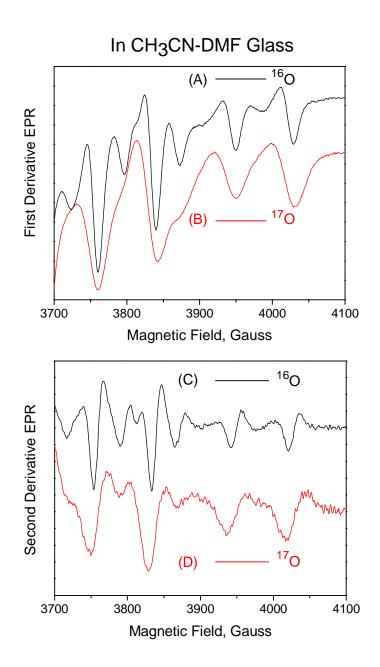
Figure 2S. The upper spectra show the first derivative X-band EPR spectra of the di-μ-oxo Mn^{III}-Mn^{IV} bipyridyl dimers exchanged with H$_2$^{16}O (A-black) and H$_2$^{17}O (B-red) in a CH$_3$CN-DMF glass. The lower spectra show the second derivative X-band EPR spectra (obtained numerically from the first derivative upper spectra by use of Origin 7.0) of the di-μ-oxo Mn^{III}-Mn^{IV} bipyridyl dimer exchanged with H$_2$^{16}O (**C**) and H$_2$^{17}O (**D**). The spectra were recorded at T = 15 K, 3 Gauss field modulation, 100 s signal averaging over a 500 Gauss field sweep, 2 mW microwave power, EPR frequency = 9.525 GHz.
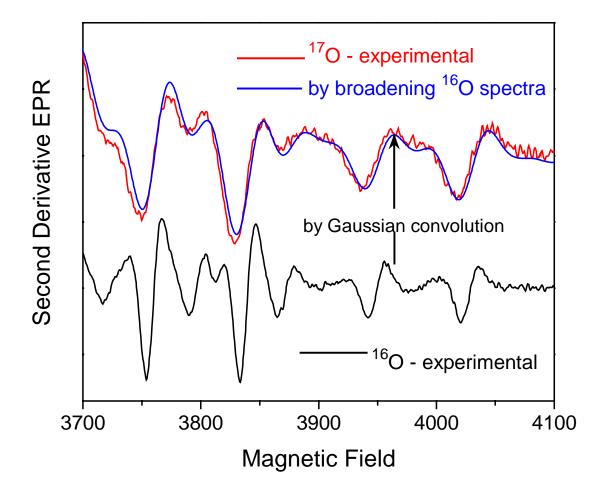
Figure 3S. The second derivative X-band EPR spectrum from the di-μ-oxo ^{17}O dimer can be obtained from the narrower line spectrum of the di-μ-oxo ^{16}O dimer by convolution of the latter with a Gaussian broadening function using the convolution tool of Origin 7.0. The black spectrum is from the sample exchanged with H_2^{16}O and the broader red spectrum is from the sample exchanged with H_2^{17}O. The blue spectrum, which approximates the broader spectrum of the di-μ-oxo ^{17}O dimer, was obtained by convoluting the spectrum of the di-μ-oxo ^{16}O dimer with a Gaussian packet line shape having a width between derivative extrema of 24 Gauss. Following Footnote 16 in the body of this Communication, the width of 24 Gauss would translate into a ^{17}O coupling of 4.96 Gauss if there are two equivalent di-μ-oxo ^{17}O giving rise to the broadening and would translate into a ^{17}O hyperfine coupling of 13.8 MHz (within experimental error of the value of $|^{17}A|$ quoted in the body of this Communication).

Part 2

In the text of the main body of this Communication the broadening due to ^{17}O was approximated by a Gaussian packet whose root mean square width between derivative extrema (Footnote 16 in the Communication) was $2A[\mathbf{n}I(I+1)/3]^{1/2} = 2\sigma$, where $I = 5/2$, $\mathbf{n} = 2$ for the di-μ-oxo configuration and A = the intrinsic ^{17}O hyperfine coupling. The formula for a Gaussian distribution is $G(x) = (2\pi\sigma^2)^{-1/2}\exp[-x^2/(2\sigma^2)]$. For two equivalent ^{17}O nuclei the true hyperfine pattern, with splitting between features of $|^{17}A|$, would be a 1:2:3:4:5:6:5:4:3:2:1 packet. If there should be only one ^{17}O contributing to the hyperfine splitting, the hyperfine pattern with splitting between features of $|^{17}A|$, would be 1:1:1:1:1:1:1.

In Figure 4SA we compare the explicit values of the Gaussian packet distribution and the 1:2:3:4:5:6:5:4:3:2:1 distribution, where the splitting between features in the latter is taken as 1 unit and where both the Gaussian and the 1:2:3:4:5:6:5:4:3:2:1 distribution will have the same root mean square width of $2\cdot[35/6]^{1/2} = 4.84$ units. The agreement between the height of features in the Gaussian packet corresponding to $\mathbf{n} = 2$ and in the 1:2:3:4:5:6:5:4:3:2:1 packet is remarkably close. Not surprisingly, simulations using the Gaussian packet and the 1:2:3:4:5:6:5:4:3:2:1 packet as broadening functions, when the two distributions have the same root mean square width, turn out to be essentially identical. In Figure 4SB we compare the explicit values of a Gaussian packet distribution and a 1:1:1:1:1:1:1 distribution, where the splitting between features of the latter is taken as 1 unit and where both the Gaussian and the 1:1:1:1:1:1:1 distribution have the same root mean square width of $2\cdot[35/12]^{1/2} = 3.42$ units. In Figure 4SB the agreement between the height of features in the Gaussian packet and in the 1:1:1:1:1:1:1 packet is at best only fair. Simulations using the 1:1:1:1:1:1:1 packet shape did not reproduce well the experimental broadening from ^{17}O.
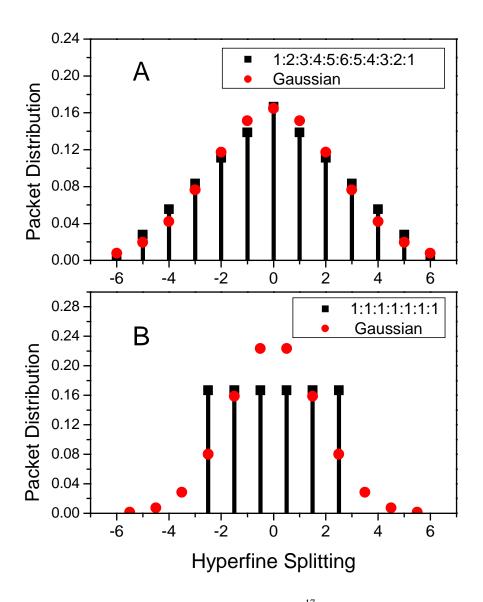
Figure 4S. In Figure **A** we compare for 2 equivalent [17]O nuclei the 1:2:3:4:5:6:5:4:3:2:1 hyperfine packet distribution to the Gaussian packet distribution corresponding to **n** = 2; where both have the same mean square width of 4.84 units. In Figure **B** we compare for one [17]O nucleus the 1:1:1:1:1:1:1 hyperfine packet distribution to the Gaussian packet distribution where both have the same mean square width of 3.42 units. It is clear that there is much better agreement between the 1:2:3:4:5:6:5:4:3:2:1 distribution and its Gaussian approximation.

In Figure 5S we compare the experimental second derivative EPR line shape of the di-μ-oxo Mn^{III}-Mn^{IV} bipyridyl dimer prepared with $H_2^{17}O$ (in black) to convolutionally broadened spectra (in red). We show data from both the CH_3CN-DMF and the CH_3CN-CH_2Cl_2 glasses; EPR hyperfine features were better resolved from the former since it was a better glass, while the ENDOR spectra (Figure 2 in the Communication) in the two glasses s were very similar. The broadened line shapes were simulated by convoluting a broadening packet (Gaussian, 1:2:3:4:5:6:5:4:3:2:1, or 1:1:1:1:1:1:1) with the narrower experimental EPR spectra of the di-μ-oxo Mn^{III}-Mn^{IV} bipyridyl dimer prepared with $H_2^{16}O$. (For the CH_3CN-DMF glass the ^{16}O di-μ-oxo Mn^{III}-Mn^{IV} bipyridyl dimer experimental EPR spectrum was that in Figure 3S; for the CH_3CN-CH_2Cl_2 glass the ^{16}O di-μ-oxo Mn^{III}-Mn^{IV} bipyridyl dimer experimental spectrum was that in Figure 1B of the body of this Communication.) For each of the simulations the underlying ^{17}O coupling was taken as 4.4 ± 0.6 Gauss, a number close to the average 4.6 Gauss reported in the Communication. For the Gaussian packet the root mean square width between derivative extrema, based on $\mathbf{n} = 2$ equivalent ^{17}O nuclei, was $= 4.84 \cdot |^{17}\mathbf{A}| = 21.3$ Gauss. It is clear that the simulations to the Gaussian and the 1:2:3:4:5:6:5:4:3:2:1 packets are virtually identical and equally effective at reproducing the ^{17}O-broadened lines shape in both glasses. On the other hand, the 1:1:1:1:1:1:1 distribution with 4.4 Gauss hyperfine coupling provides insufficient broadening in the convolution process to simulate the ^{17}O spectra in either glass. We conclude that the hyperfine coupling which accounts for the ENDOR ^{17}O results will only account for the EPR broadening if there are two contributing equivalent di-μ-oxo ^{17}O, but not one ^{17}O. We further conclude that the Gaussian approximation corresponding to $\mathbf{n} = 2$ and the 1:2:3:4:5:6:5:4:3:2:1 packet work equally well where both represent coupling to two equivalent ^{17}O.

For completeness in our simulation of broadening, we also attempted, as shown in Figure 6S, to simulate the EPR line broadening using a ^{17}O hyperfine coupling of 5.9 Gauss (= 16.4 MHz) which was larger than that observed by ENDOR. This simulation if used for two equivalent ^{17}O and a 1:2:3:4:5:6:5:4:3:2:1 packet, produced a line shape which was broader and less detailed than the experimental line shape of the di-μ-oxo Mn^{III}-Mn^{IV} bipyridyl dimer prepared with H$_2$^{17}O. The simulation when used with one ^{17}O and a 1:!:1:1:1:! packet did not fit features and led to experimentally non-observed shoulders, especially in the CH$_3$CN-DMF glass.

CH₃CN-DMF Solvent
¹⁷O coupling = 4.4 G

A — di-μ-oxo ¹⁷O / convolution — Gaussian

B — 1:2:3:4:5:6:5:4:3:2:1

C — 1:1:1:1:1:1

CH₃CN-CH₂Cl₂ Solvent
¹⁷O coupling = 4.4 G

D — di-μ-oxo ¹⁷O / convolution — Gaussian

E — 1:2:3:4:5:6:5:4:3:2:1

F — 1:1:1:1:1:1

Second Derivative of EPR spectra
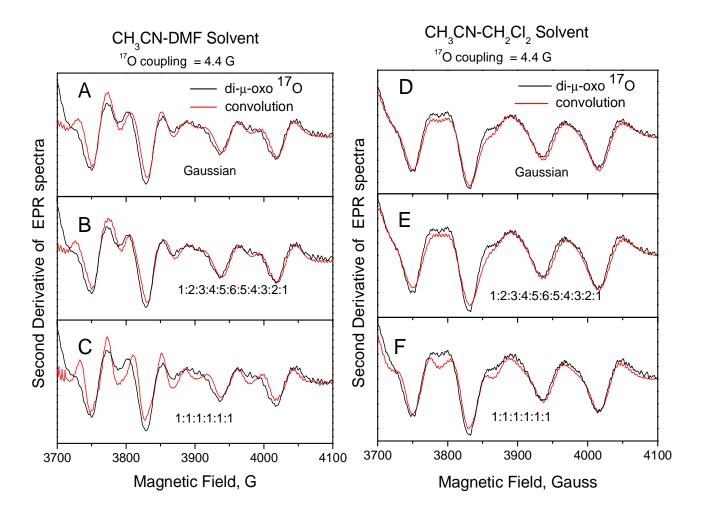
Magnetic Field, G — Magnetic Field, Gauss

Figure 5S. In this figure we compare the experimental second derivative features from the di-μ-oxo Mn^{III}-Mn^{IV} bipyridyl dimer prepared with $H_2^{17}O$ to simulated spectra. The simulated spectra were obtained by convoluting the packet shape indicated on each spectrum with the experimental narrower line spectrum of the di-μ-oxo Mn^{III}-Mn^{IV} bipyridyl dimer prepared with $H_2^{16}O$. (For the CH₃CN-DMF solvent the ^{16}O di-μ-oxo Mn^{III}-Mn^{IV} bipyridyl dimer experimental spectrum is that in Figure 3S; for the CH₃CN-CH₂Cl₂ solvent the ^{16}O di-μ-oxo Mn^{III}-Mn^{IV} bipyridyl dimer experimental spectrum is shown in Figure 1B of the body of this Communication.) The ^{17}O hyperfine coupling of 4.4 Gauss used was comparable to the average value of 4.6 ± 0.6 Gauss reported in the Communication and also consistent with the ENDOR results. As indicated by spectra A, B, D, E the experimental features in both solvents were well simulated by either the Gaussian or the 1:2;3:4:5:6:5:4:3:2:1 packet from two equivalent ^{17}O, each with a ^{17}O hyperfine coupling of 4.4 Gauss. As indicated in Spectra C and F the 1:1:1:1:1:1 packet from one ^{17}O with a hyperfine coupling of 4.4 Gauss showed sharper peaks than were observed.
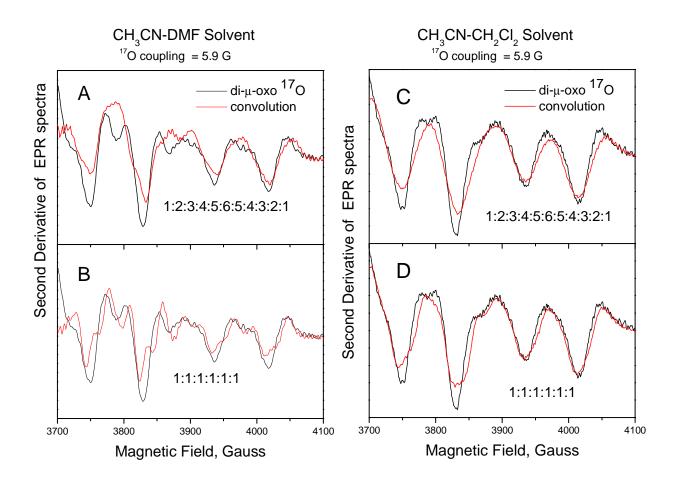
Figure 6S. In this figure we have simulated the broadening due to ^{17}O by using a larger coupling of 5.9 Gauss (= 16.5 MHz) than is consistent with ENDOR results, to determine whether ^{17}O with a larger coupling might be used to simulate the ^{17}O-brodeneed spectra. (For the CH_3CN-DMF solvent the ^{16}O di-μ-oxo Mn^{III}-Mn^{IV} bipyridyl dimer experimental spectrum is that in Figure 3S; for the CH_3CN-CH_2Cl_2 solvent the ^{16}O di-μ-oxo Mn^{III}-Mn^{IV} bipyridyl dimer experimental spectrum is shown in Figure 1B of the body of this Communication.) Convolution with the 1:2:3:4:5:6:5:4:3:2:1 packet due to two equivalent ^{17}O over-broadened all features so that the fits were poorer than those than those on the previous page with a hyperfine coupling of 4.4 Gauss. The 1:1:1:1:1:1 packet corresponding to one ^{17}O with a coupling of 5.9 Gauss did not fit features near 3800 Gauss in Spectrum D and led for the CH_3CN-DMF glass to the appearance of additional shoulders in Spectrum B that were not experimentally observed.

References

1. Cooper, S. R.; Dismukes, G. C.; Klein, M. P.; Calvin, M. *J. Am. Chem. Soc.* **1978**, *100*, 7248.

2. Randall, D. W.; Sturgeon, B. E.; Ball, J. A.; Lorigan, G. A.; Chan, M. K.; Klein, M. P.; Armstrong, W. H.; Britt, R. D. *J. Am. Chem. Soc.* **1995**, *117*, 11780.